Soft Matter

Soft Matter Emerging Investigators Issue 2021: Phase mechanics of colloidal gels: osmotic pressure drives non-equilibrium phase separation

Journal:	*Soft Matter*
Manuscript ID	SM-ART-12-2020-002180.R1
Article Type:	Paper
Date Submitted by the Author:	20-Jan-2021
Complete List of Authors:	Johnson, Lilian; Stanford University, Chemical Engineering Zia, Roseanna; Stanford University, Chemical Engineering

Journal Name

ARTICLE TYPE

Cite this: DOI: 00.0000/xxxxxxxxxx

Phase mechanics of colloidal gels: osmotic pressure drives non-equilibrium phase separation

Lilian C. Johnson and Roseanna N. Zia*

Received Date
Accepted Date

DOI: 00.0000/xxxxxxxxxx

Although dense colloidal gels with interparticle bonds of order several kT are typically described as resulting from an arrest of phase separation, they continue to coarsen with age, owing to the dynamics of their temporary bonds. Here, k is Boltzmann's constant and T is the absolute temperature. Computational studies of gel aging reveal particle-scale dynamics reminiscent of condensation that suggests very slow but ongoing phase separation. Subsequent studies of delayed yield reveal structural changes consistent with re-initiation of phase separation. In the present study we interrogate the idea that mechanical yield is connected to a release from phase arrest. We study aging and yield of moderately concentrated to dense reversible colloidal gels and focus on two macroscopic hallmarks of phase separation: increases in surface-area to volume ratio that accompanies condensation, and minimization of free energy. The interplay between externally imposed fields, Brownian motion, and interparticle forces during aging or yield changes the distribution of bond lengths throughout the gel, altering macroscopic potential energy. The gradient of the microscopic potential (the interparticle force) gives a natural connection of potential energy to stress. We find that the free energy decreases with age, but this slows down as bonds get held stretched by glassy frustration. External perturbations break just enough bonds to liberate negative osmotic pressure, which we show drives a cascade of bond relaxation and rapid reduction of the potential energy, consistent with renewed phase separation. Overall, we show that mechanical yield of reversible colloidal gels releases kinetic arrest and can be viewed as non-equilibrium phase separation.

1 Introduction

Colloidal gels are soft solids that can fluidize under external fields and forces, and then regain solid-like character when such fields are removed. This behavior has been leveraged for a multitude of applications in the pharmaceutical, personal-care, food, and petroleum industries as a means by which to store compounds in the solid-like scaffold and then permit flow to deliver them for injection, surface application, and extraction applications. Such gels comprise microscopically small particles, often idealized as spheres, disks, plates, or rods, that bond together into solvent-suspended networks.

Gelation can be induced through a combination of particle volume fraction and interparticle bonds that together provide both connectedness and rigidity, in a process that typically involves inducing attractions at a given volume fraction. Several routes through the gelation process have been described in the literature, well summarized by Zaccarelli[1]. The bonds between particles arise from an interparticle potential V that ranges from just a few kT to hundreds of kT, depending on the origin of the attractions (here, k is Boltzmann's constant and T is the absolute temperature). Strong, fractals gels form by diffusion-limited aggregation[2] and are favored in dilute systems where $V \gg kT$, often induced by the addition of salt. The bonds in such gels can be described as permanent because thermal fluctuations are very rarely strong enough to break a bond; external flow or forces can of course rupture the bonds and fluidize the gel. The mechanical properties of these 'permanent' gels are well-described by, e.g., fractal scaling[2–5] or poroelastic theory[6–8]. In contrast, when attractions between particles are on the order of just a few kT, gelation of a moderately concentrated to dense suspension produces a non-fractal bi-continuous morphology in which particle bonds frequently rupture and reform due to thermal fluctuations[9,10]. Such bonds are induced by the addition of non-adhering depletant polymer or adhering bridging chains[11,12]. We describe these as 'reversible' gels to highlight the prominent role played by frequent thermal bond rupture in quiescent aging. Particle diffusion is quite dominant in the gelation process of reversible gels: when V is only several kT, the attractions that promote phase separation also inhibit it, by slowing the Brownian motion of par-

Department of Chemical Engineering, Stanford University, Stanford, CA, USA.
* Email: rzia@stanford.edu

ticles as they attempt to condense together. At sufficiently high volume fraction, e.g. above about 20%, gelation occurs via arrested phase separation, resulting in dense, thick strands of particles that are connected via durable but transient bonds.[9–14] This competition between Brownian and interparticle forces allows gels to restructure over time – they age coarsen,[14–17] which impacts their mechanical behavior[14,18]. The reversibility of interparticle bonds also underlies the utility of such gels, permitting on-demand liquid-to-solid transitions and self-healing properties. But bond reversibility also underpins problems with aging[14] and mechanical instability that can be difficult to predict. Examples include delayed yield and delayed re-solidification under fixed shear stress[19–22] and gravitational collapse[15,23,24]. Equilibrium theory cannot explain mechanistically the microscopic origins of these behaviors. To address the impact of these problems on the personal care, pharmaceutical, and food industries, the last decade has seen a strong focus on understanding aging and the time-dependent behavior of dense, reversible colloidal gels. In our recent work[14,22,24,25] we have suggested that phase arrest can vary in depth and that mechanical yield is connected to a release from this arrest.

While macroscopically, phase separation in reversible colloidal gels appears to be arrested, recent computational study of detailed particle dynamics within the gel reveals that an equilibrium-like process persists: colloids on the exterior surface of the gel undergo a rapid exchange process between the surface and solvent.[14] We have proposed that this condensation process should be viewed as part of ongoing phase separation.[14] Over time, the particles that condense onto the surface seek additional bonds by diffusing along the curvy network surface, eventually becoming permanently condensed deep within the gel strands. The same simulation study showed that the coarsening process occurs via diffusive migration, where particles are ratcheted into deeper energy states as they acquire more bonds. The natural connection between bondedness and potential energy suggests that coarsening is an energy minimization process, where particles seek more contacts in order to reduce their potential energy. Despite this ongoing structural evolution, however, the rate of coarsening migration never reaches asymptotic scalings predicted by molecular theory,[26,27] and full phase separation does not occur. From this we developed the idea is that aging in reversible colloidal gels is ongoing but very slow phase separation, which leads naturally to the question of whether external perturbations such as shear or gravity could release arrest to allow rapid phase separation to re-emerge.

Our subsequent study of the delayed yield of reversible colloidal gels revealed a connection of yield to restarted phase separation.[22] Depending on the strength of the imposed stress, gels might never yield, or might fluidize and flow after a delay. When subjected to a rather weak stress, a gel can actually re-solidify during flow, with no change in applied stress. In contradiction to the idea that these behaviors resulted purely from advective rearrangements, we found they are most likely to occur when applied stress is much weaker than kT. In fact, thermal forces were shown to facilitate yield rather than heal the gel, pointing toward a reactivation of the phase separation process, where the role of the weak external stress was simply to trigger the ensuing condensation. Microscopic analysis was consistent with this picture: inspection of bond dynamics revealed the surprising result that there was little net bond loss at yield. Although appreciable bond loss accompanies fluidization well after the yield, at long times there is a reversal from net bond loss to net bond gain occurring at the same time as macroscopic rheological re-solidification, at which point the gel is more condensed. These bond dynamics provide an important link to macroscopic total energy: one hallmark of equilibrium phase separation is a reduction in free energy and in a colloidal system, which includes the potential energy of bonds and the thermal energy of Brownian motion. In the study of delayed shear yield, the rate of reduction of potential energy during the re-solidification was faster than that in a quiescently aging gel, supporting the idea that delayed shear yield is re-activated phase separation. Signals of activated release from arrest can also be found in the stress overshoots and subsequent condensation of a gel subjected to an imposed shear rate.[25] The next logical step is to identify the driving force that is evidently "locked away" in the arrested gel but is liberated by a weak external perturbation.

Our more recent study of the gravitational collapse of colloidal gels revealed osmotic pressure as the driving force for the rapid bulk condensation that takes place during rapid collapse.[24] Similar to the delay in fixed-shear stress and the startup regime in fixed-strain rate experiments, gravitational collapse of colloidal gels begins with an almost imperceptibly slow compaction period followed by a sudden transition to rapid collapse. We found that yield occurs at a tipping point at which the loss of a few interparticle bonds permits a cascade of bond relaxation within the gel. The difference between compaction and collapse was distinguished by measurements of osmotic pressure. In the bulk of the gel, away from boundaries, enhanced coarsening drives densification, and detailed interrogation of particle-phase stress revealed the origin to be negative osmotic pressure: stretched interparticle bonds relax, pulling the gel inward on itself. Rapid collapse is not purely compaction; coarsening orthogonal to gravity suggests phase separation instead. That is, densification arises not only due to particle advection toward the container bottom, but initially and principally due to negative osmotic pressure. Together these suggest a non-equilibrium reactivation of phase separation driven by interparticle attractions. The role of gravity is to activate the release from kinetic arrest allowing condensation and phase separation to proceed. Counterintuitively, gravity actually acts to stop collapse: once many bonds relax and some compress, the gel re-arrests, preventing complete phase separation. Thus, this study of gravitational collapse revealed osmotic pressure – not gravity – as the driving force of reactivated phase separation that further condenses the gel, which ends when osmotic pressure reverses sign from negative to positive.

These findings suggest that osmotic pressure drives, and does not just accompany, release from kinetic arrest, revealing the intriguing possibility that phase separation can be reactivated in a deeply arrested gel. Here, we aim to expand the thermodynamic connection between osmotic pressure and equilibrium phase separation to a kinetic role in non-equilibrium phase sepa-

ration by showing the same connections in quiescently aging gels, and those yielding under fixed shear stress and fixed strain rate. We restrict our hypotheses and conclusions to the regime of moderately concentrated hard-sphere colloidal gels, $0.20 \leq \phi \leq 0.45$, where ϕ is the particle volume fraction, where attractions are short ranged $10-20\%$ of particle diameter or less) and bonds are characterized by a single minimum not greater than $15kT$, which we have studied in our previous work[14,22,24,25,28].

The remainder of this paper is organized as follows: The model system and dynamic simulation methods are presented in Section 2. In Section 3, we define the osmotic pressure and describe its connection to interparticle forces, phase behavior, and free energy minimization. The results, Section 4, are organized in several studies where we review the rheological, structural, and microscopic behavior of the colloidal gel and the accompanying osmotic pressure evolution: quiescent aging in Section 4.1, gravitational collapse in Section 4.2, delayed yield under a step shear stress in Section 4.3, and startup of a fixed strain rate in Section 4.4. A micromechanical picture of osmotic pressure is presented in Section 4.5. The conclusions are presented in Section 5.

2 Methods

2.1 Model system

Our model colloidal gel comprises a suspension of hard Brownian spheres of radius a. The particles are neutrally buoyant, except when gravitational forcing is applied, which we address later. The surrounding fluid is treated as a continuum with viscosity η and density ρ. Fluid motion is governed by Stokes' equations due to the vanishingly small Reynolds number associated with colloidal size, $Re = \rho U a/\eta$, where U is the characteristic particle velocity. The volume fraction of particles $\phi \equiv 4\pi a^3 n/3$ (where n is the number density of particles) utilized here is $\phi = 0.2$ and is sufficiently large to form a network when particle interactions are reversible. Such volume fractions are also pertinent to colloidal gels studied via experimental rheology and microscopy, which often exhibit the same characteristic time-dependent behavior of reversible bonds.[11–13,18,19,28,29] Particles exert a hard-sphere repulsion at contact and hydrodynamic coupling is neglected. Attractions between particles, as would arise from the exclusion of a smaller species from the space between two colloidal particles, are modeled. This depletion interaction[30] is widely utilized in experimental systems.[11,12,16–18,28] We introduce this as a short-ranged attraction of strength $O(kT)$, which permits thermal motion to play a role in the formation and rupture of bonds between particles arising from the attractive force. This interparticle potential $V(r)$ is well-represented by the Morse potential, which provides a steep, hard-sphere repulsion and short-ranged attraction,

$$V_{ij}(r_{ij}) = -V_0\left(2e^{-\kappa[r_{ij}-(a_i+a_j)]} - e^{-2\kappa[r_{ij}-(a_i+a_j)]}\right), \qquad (1)$$

where r_{ij} is the center-to-center distance from particle i to particle j. The characteristic well depth V_0, the exponent κ, and the interparticle distance between particles $a_i + a_j$ are adjusted to set the attraction range, attraction well depth, and particle polydispersity, given by particle sizes a_i and a_j. The range of the attraction, $\kappa = 30/a$, approximates a polymer-to-colloid size ratio of 0.1 (Figure 1). To model a reversibly bonded system, $V_0 = 5$, $6\ kT$ to enable structural evolution under quiescent conditions. Polydispersity is introduced by a distribution of particle radii a_i of 7% (relative standard deviation) to suppress crystallization, and is commonly realized in experimental systems.[31]

Reversible colloidal gels are challenging to simulate due to the large system size required to provide sufficient sampling of the many length scales and time scales present. To mitigate finite-size effects, we formed the gel from 750,000 particles, replicating it periodically to focus on bulk rather than boundary effects, except in the gravitational collapse study, where the top and bottom of a container are essential to probing collapse. We construct the simulation using the LAMMPS molecular dynamics package[32]. Gels are aged $40a^2/D$ to $400{,}000a^2/D$; external forcing is then applied.

2.2 Dynamic simulation

Colloidal particle motion is set by the Langevin equation,

$$\mathbf{m}\cdot\frac{d\mathbf{U}}{dt} = \mathbf{F}^H + \mathbf{F}^B + \mathbf{F}^P, \qquad (2)$$

where $\mathbf{m}$ is the mass or moment of inertia tensor and $\mathbf{U}$ is the particle velocity. The forces which act upon each particle are hydrodynamic $\mathbf{F}^H$, Brownian $\mathbf{F}^B$, and interparticle $\mathbf{F}^P$ forces. A drag force is applied as $\mathbf{F}_i^H = -6\pi\eta a_i[\mathbf{U}_i - \mathbf{U}^\infty(\mathbf{x}_i)]$, determined for particle i by its velocity $\mathbf{U}_i$ relative to the background solvent viscosity $\mathbf{U}^\infty$ at the particle center $\mathbf{x}_i$. A Brownian or stochastic force models the numerous collisions of solvent molecules with the colloidal particle giving rise to Brownian motion,

$$\overline{\mathbf{F}_i^H} = 0, \qquad \overline{\mathbf{F}_i^B(0)\mathbf{F}_i^B(t)} = 2kT(6\pi\eta a_i)\mathbf{I}\delta(t), \qquad (3)$$

where $\mathbf{I}$ is the identity matrix and overbars denote time averages. These solvent kicks are correlated instantaneously and follow Gaussian statistics. The interparticle force $\mathbf{F}^P$ between each pair of particles is determined from the Morse potential (**Equation 1**),

$$\mathbf{F}_i^P = -\sum_j \frac{\partial V_{ij}(r_{ij})}{\partial r_{ij}}\hat{\mathbf{r}}_{ij}, \qquad (4)$$

where $\hat{\mathbf{r}}_{ij}$ is a unit vector along the line of centers of particles i and j. Particle trajectories are computed via velocity-Verlet integration[33] and a Langevin thermostat[34] in the LAMMPS molecular dynamics simulation package.[32] We ensure that the effect of particle inertia is sufficiently small to recover Stokesian physics by enforcing a small Stokes number, $St = (\rho_p/\rho_f)Re \ll 1$, where ρ_p and ρ_f are the particle and fluid density, which requires of a suitably small time step of integration[14]. The time over which the system evolves is made dimensionless on the Brownian time scale, a^2/D, where $D = kT/6\pi\eta a$ is the lone-particle diffusion coefficient. Results of this model system and simulation method capture the physics of inertia-free systems[35] over the range of shear rates examined within this work.

To prepare the gel, the simulation cell is populated with the colloids randomly distributed in space, and the dynamics are initiated. Brownian diffusion and displacements due to the interparticle potential induce arrested phase separation and subsequent

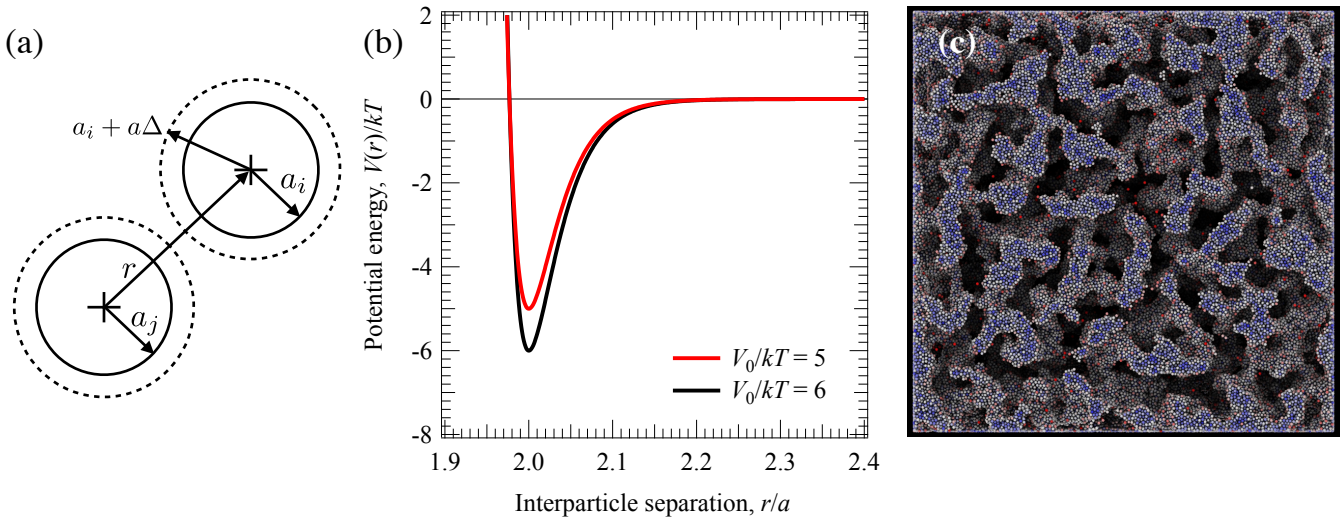

Fig. 1 (a) Model system with, for example, particles of size a_i and a_j and interparticle separation r which interact over a range given by Δ. (b) Morse potential $V(r)/kT$ with range parameter $\kappa = 30/a$ and depth of $V_0 = 6kT$ as a function of separation distance between two particles, of average particle radius a. (c) Snapshot of a quiescently aged gel with $5kT$ interparticle attraction strength at an age of $40{,}000a^2/D$.

ongoing aging, as described in detail in Zia *et al.*[14] In this work, we examine both quiescent conditions, and quiescently-aged gels subjected to gravitational forcing, step stress, and startup of shear flow. The simulation method for each technique is covered in more detail elsewhere[22,24,25]; here we summarize the main features of imposing external forcing.

Gravitational forcing is applied as a body force to the particles, to mimic the net force that arises when the density of colloidal particles and solvent differ as $\Delta\rho$, e.g. the particles are not neutrally buoyant. To do so, a quiescently-aged gel is placed between two parallel walls for a short time before the gravitational body force g is applied to the particles. The body force is incorporated into the Langevin equation Equation 2, as presented in Padmanabhan and Zia.[24] The strength of gravity relative to the Brownian force gives a gravitational Péclet number, $Pe_g = 4\pi\Delta\rho g a^4/3kT$. Now, particles will sediment during gelation, especially those that are substantially more dense than the suspending solvent and could lead to a gel that is more dense on the bottom, which could influence subsequent collapse dynamics. This scenario of very heavy particles goes hand in hand with the fact that a gel can always be forced to collapse under strong external forcing (high density ratio). However, we are not interested in this regime, because it is of lesser importance to the vast number of industrial applications where sudden gel collapse is an ongoing challenge. The most interesting and troublesome cases of gravitational collapse are observed in gels made from particles that are just barely non-neutrally buoyant that seem to support their own weight for long periods before suddenly collapsing. We conducted side-by-side simulations of sedimentation of a purely repulsive system of colloids, and found that sedimentation is far slower than the time required for our gel to form. Once formed, however, gel collapse is much faster than sedimentation owing to the negative osmotic pressure within the gel[24]. The boundary conditions include a container top and bottom that experience the doubled attraction with the colloids[36], and is infinite in extent in the directions orthogonal to gravity. Although side walls do resist the action of gravity on a gel, Starrs *et al.* conducted a study of the impact of container walls on the gel collapse phenomenon, and found that sufficiently wide containers exhibit identical delay times[23]. Our results are thus strictly valid for containers that are not too narrow.

Step stress is applied to a gel at a given age via a mechanism inspired by the Nosé-Hoover feedback mechanism;[37] this method is reviewed here, and details can be found in Landrum *et al.*[22] The method deforms periodic system in the xy-plane at a rate that produces the desired set point shear stress, responding to offsets in the shear stress σ_{xy} by varying the imposed strain rate $\dot{\gamma}$. The strength of the imposed shear can be made dimensionless to form a Péclet number as $Pe_\sigma \equiv (\sigma_{xy}/\eta)a^2/D = 6\pi a^3\sigma_{xy}/kT$. Startup shear flow is applied to a periodic system by imposing a linear velocity field $\mathbf{U}^\infty(\mathbf{x}) = \dot{\gamma}y$; $\dot{\gamma}$ is the shear rate and y is the direction of the velocity gradient. A Péclet number is defined as $Pe_{\dot{\gamma}} \equiv \dot{\gamma}a^2/D$, giving the ratio of the shear rate to the rate of diffusion; a range of $0.005 \leq Pe \leq 1$ is examined here, a range comparable to strain rates utilized in experiments.[18]

3 Osmotic pressure, stress, energy density, and free energy

The total stress and its individual contributions can be viewed as the energy density of a colloidal system, as seen by the units of stress: $Nm/m^3 = N/m^2$. The particle-phase stress includes the ideal osmotic pressure $-nkT\mathbf{I}$, the interparticle stress $n\langle\mathbf{r}\mathbf{F}^P\rangle$, and the hydrodynamic stress $\langle\boldsymbol{\Sigma}\rangle^H$:

$$\langle\Sigma\rangle = -nkT\mathbf{I} - \langle\mathbf{r}\mathbf{F}^P\rangle + \langle\Sigma\rangle^H. \quad (5)$$

Here, $\mathbf{I}$ is the identity tensor, r is the particle position, and the angle brackets indicate an average over all particles. The hydrodynamic stress includes contributions due to externally imposed flow, Brownian disturbance flows, and dissipative contributions

from interparticle forces. In a freely draining suspension, this term is absent but particle displacements arising from imposed flow, fields, or forces lead to particle displacements that produce interparticle stress. The osmotic pressure contribution from interparticle interactions Π^P is a scalar quantity related to the trace of the stress tensor arising from the interparticle stress:

$$\Pi^P = -\mathbf{I} : \mathbf{\Sigma}^P/3 \tag{6}$$

The osmotic pressure is one way to quantify the tendency of a colloidal system to expand or condense, as illustrated in Figure 2.

When the osmotic pressure is positive, e.g. as with a suspension of purely-repulsive colloidal hard spheres, Brownian diffusion drives the particles to continuously explore a larger volume of space over time, exerting a positive force on the walls of a fictitious surrounding container, Figure 2(b). When attractive forces are present, the osmotic pressure can become negative, condensing the system inward, Figure 2(a). During gelation, bonds form between particles and the newly-formed state comprises many stretched bonds. Each bond contributes at the microscopic level to the macroscopic osmotic pressure, and an abundance of stretched bonds gives macroscopic negative osmotic pressure. Newly formed bonds can relax and subsequently stretch or compress; in the case of an initially dispersed system, formation of many bonds is needed to produce equilibrium phase separation and results in a condensed phase. Certain bond strengths can also interrupt equilibrium phase separation, producing a colloidal gel. In this work, we study the role played by osmotic pressure in the evolution of colloidal gels under quiescent conditions and when subjected to external forces, with a view toward understanding arrested phase separation.

The interplay between externally imposed stress, Brownian motion, and interparticle forces alters the potential energy of the gel, which is an average $\langle V \rangle$ of the potential energy from all bonds in the gel, each of which is given by $V(r)$. Thus, the interparticle force derivable from that potential, $\mathbf{F}^P = -\nabla V$, connects the stress with the gel's potential energy. The interplay between microscopic forces also changes the particle configuration, relating flow energy to entropic energy. The free energy of the gel can be written $\langle F \rangle = \langle V \rangle - TS$, and quantifies how changes in microstructure arising from flow or gel aging can change the gel's free energy, where $\langle F \rangle$ is the free energy and S is the entropy. Flow or imposed stress can stretch bonds, increasing gel stress and changing its free energy. The push to minimize this free energy is carried out by the osmotic pressure, acting to relax bonds, which itself has a clear connection to thermodynamic variables. Owing to the slowed dynamics in a colloidal gel, the connection of mechanical stress and yield to free energy and phase separation can be made via the osmotic pressure.

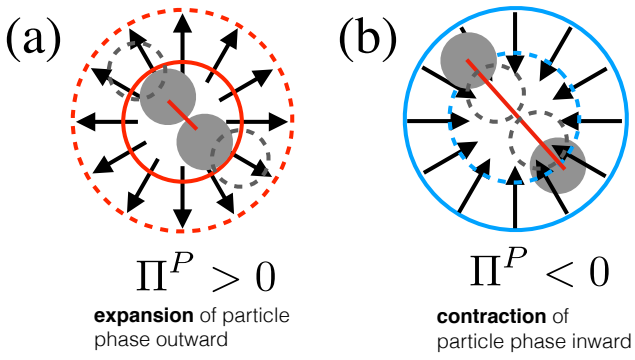

Fig. 2 Illustration of the osmotic pressure in a colloidal suspension.

4 Results

Here we report new results from the study of the osmotic pressure evolution in several examples of evolving colloidal gels: under quiescent conditions and subjected to perturbation from external fields, forces, and imposed deformation. We begin with analysis of a quiescently aging gel to establish a baseline from which to understand the ongoing process of condensation and re-initiated condensation following yield.

4.1 Quiescently aging colloidal gels

Age coarsening has been shown to persist in colloidal gels long after gelation.[15–17,38] Gel aging involves an ongoing growth in characteristic network length scale defined by thick particle strands and solvent pores, which leads to age stiffening of their rheological response.[14] In our prior work, we found that the interior of gel strands is glassy: the volume fraction inside strands is about $\phi = 0.62$ which, combined with a logarithmic decay of the intermediate scattering function, indicates an attractive glass. The density deep in the strands does not change with age; rather, coarsening involves growth of the volume of dense condensed regions. This aging process takes place quiescently, where the only forces present are the Brownian force, which tends to diffuse particles away from each other, and interparticle forces, which tends to pull particles together to form bonds. We showed that the temporal growth rate of the network length scale is always much smaller than molecular theories predict for coalescence or ripening, and thus suggested that the rate of coarsening is "slow" and arises from non-equilibrium mechanisms not describable via equilibrium phase separation theory.

Instead, we view the coarsening that is carried out by surface diffusion of individual colloids along the network[14] as an ongoing non-equilibrium phase separation mechanism that is specific to colloidal gels. A large fraction of the colloids in these dense gels are sterically frozen deep inside network strands; only surface particles play an active role in in ongoing coarsening (see Figures 11 and 12, Zia et al[14]). The resulting increase in interior strand volume at fixed overall volume fraction occurs concomitant with a decrease in surface area, a macroscopic indictor of an ongoing phase separation process. The shift to higher particle number is also consistent with the idea of ongoing phase separation in that it indicates a slow ratcheting of particles into more bonded, deeper-energy states.[14] The natural next step is to discover the specific driving force that is reducing the free energy of the gel, one that does so by formation and relaxation of interparticle bonds. The gel's average potential energy is connected to the gel's free energy

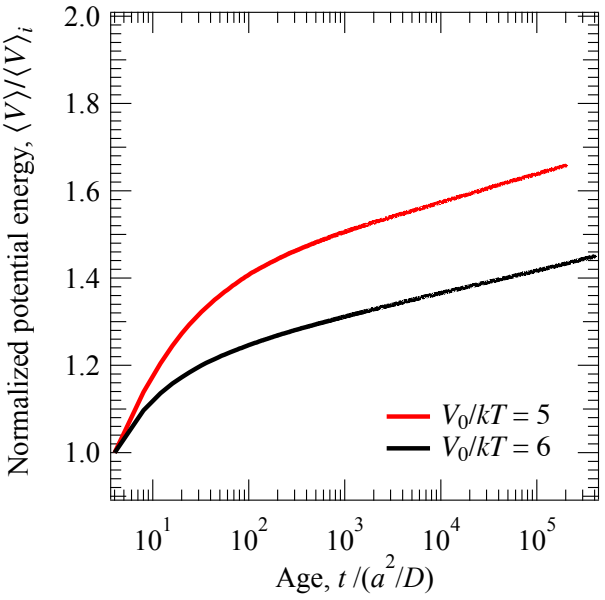

Fig. 3 Potential energy normalized on its value $\langle V\rangle_i$ at a gel age of 4 a^2/D as a function of gel age for gels of attraction strength 5 and $6kT$.

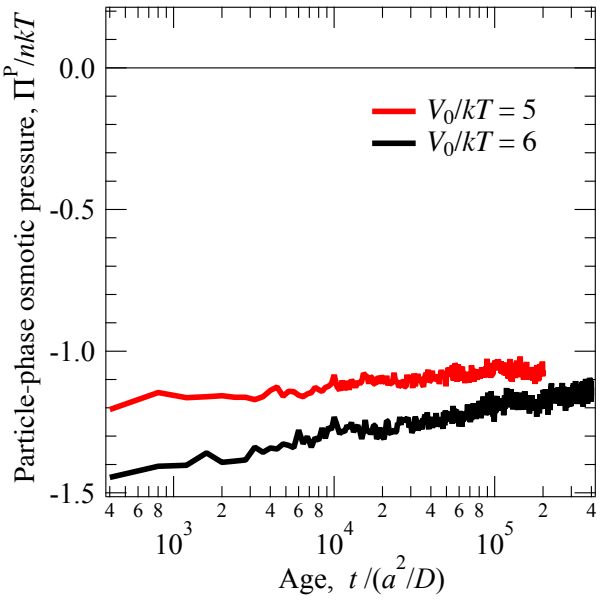

Fig. 4 Particle-phase osmotic pressure as a function of gel age in quiescently aging gels of attraction strength 5 and $6kT$.

(cf Section 3), and is relevant because free energy minimization is a feature of phase separation.

In the present study, we measured the gel's evolving potential energy as it aged, by monitoring the formation, loss, stretching, compression, and relaxation of each bond and computing its total as an average over all bonds. Bonds tend to form in the stretched state (at the maximum potential well width), and subsequently evolve due to the ongoing interplay between the $O(kT)$ Brownian force and the $5kT$ or $6kT$ attractive force that allows particles to sample the strand surface where they can acquire new bonds. Condensation occurs microscopically when the interparticle potential and its gradient drive many particles deeper into these wells. As a result, we expect that the ongoing formation of new bonds and relaxation of existing bonds will drive the potential energy lower (more negative) which will make the ratio to its initial value, $\langle V\rangle/\langle V_0\rangle$, grow above unity. To interrogate this idea, we measured average potential energy in simulations throughout the gel's evolution. The normalized potential energy $\langle V\rangle/\langle V_0\rangle$ is plotted in Figure 3. The normalized potential energy grows above unity over all ages, indicating that free energy minimization is ongoing and driven by the formation and relaxation of many bonds. Owing to the fundamental connection between free-energy minimization and equilibrium phase separation, Figure 3 provides further support for the idea that a slow, non-equilibrium phase separation takes place as the gel coarsens quiescently.

While the reduction of free energy is the underlying thermodynamic goal of phase separation, the bond relaxation needed to reduce the potential energy in a gel is frustrated by deep steric hindrance within gel strands, i.e., dynamic arrest. However, arrest is not total, as evidenced by ongoing restructuring, coarsening, and slow energy evolution; we thus infer that there must be a driving force that continues to push toward phase separation despite deepening arrest, which we look for next.

Throughout a colloidal gel, there will be a distribution of many different bond states, from stretched to relaxed to compressed; the microscopic driving forces acting through each of these individual bonds thus ultimately act collectively to produce an average or macroscopic driving force for condensation: the osmotic pressure. Whereas the overall macroscopic free energy (the collective effect of the microscopic potential) is the "state variable" we are tracking and is a signal of phase separation, the macroscopic osmotic pressure arises as the collective effect of *gradients* of the microscopic potential energy, and is the driving force for phase separation. The potential energy has a value at each instant in time that cannot predict whether the gel is going to change, but because the osmotic pressure directly encodes a gradient of the potential, it does predict whether the gel is evolving. The non-equilibrium osmotic pressure is, in a sense, an arrested macroscopic driving force toward continued phase separation.

The osmotic pressure reflects the fact that phase separation takes place on the microscopic level through evolution of individual bonds to minimize free energy. We measured the osmotic pressure for a quiescently aging gel and plotted it as a function of age in In Figure 4. We find that the osmotic pressure is negative over all gel ages, which is associated with condensation (cf Section 3). This is consistent with changes in $P(N_c)$, $L_{S(q)}$, $P(\phi)$, and $\langle V\rangle$ [14] that together indicate that negative osmotic pressure drives bond relaxation and thus reduction in potential energy that permit ongoing phase separation. Notably, the osmotic pressure weakens with time, suggesting that ongoing coarsening slows down: it is self-limiting, owing to structural evolution and bond relaxation that reduce the drive to condense, suggesting a flattening energy landscape, and that there is not a quiescently accessible equilibrium state.

Our previous study of gel yield [22,24,25] suggested that an external perturbation can re-initiate phase separation, and in our study

of gel collapse we found that osmotic pressure is the driving force. We now look back and ask if the osmotic pressure can be generalized as the driving force for non-equilibrium phase separation.

4.2 Gravitational collapse of colloidal gels

Gel collapse is a striking phenomenon where a seemingly stable, space-spanning gel network suddenly and rapidly collapses into a sediment, observed first via experiment [15] and first modeled via large-scale simulation by our group [24]. Gravitational collapse is influenced by particle volume fraction, the strength of interparticle bonds, and of course the density difference between particles and solvent. The last of these sets the strength of gravitational forcing. Very heavy particles may sediment as they gel, after which the newly formed gel collapses. This scenario of very heavy particles goes hand in hand with the fact that a gel can always be forced to collapse under strong external forcing (high density ratio). However, we are not interested in this regime, because it is of lesser importance to the vast number of industrial applications bedeviled by sudden gel collapse. The most interesting and troublesome cases are observed in gels made from particles that are just barely non-neutrally buoyant that seem to support their own weight for long periods before suddenly collapsing (see discussion in §2).

Gel collapse manifests macroscopically as bulk sedimentation that begins at a very slow rate, then undergoes an abrupt transition to rapid sedimentation, and is then followed by slow, long-time compaction. Our models include a container top and bottom that experience the doubled attraction with the colloids, and is infinite in extent in the directions orthogonal to gravity. We neglect side walls, which would resist the action of gravity on a gel; however, Starrs *et al.* conducted a study of the impact of container walls on the gel collapse phenomenon, and found that sufficiently wide containers exhibit identical delay times [23]. Our results thus pertain to gels in containers that are not too narrow. We found in our previous study that changes in the osmotic pressure drive the different regimes of gravitational collapse. [24] This picture emerges from analysis of bond dynamics, coarsening rate, potential energy, and structural evolution. Gravity simply kicks off the process by rupturing a few bonds, allowing many other to relax and many more new bonds form as the gel densifies. The osmotic pressure drives this process: it is initially strongly negative, then weakens during rapid collapse as bonds relax. The osmotic pressure is strongest (most negative) at the onset of the rapid collapse phase: there are many stretched bonds that then begin to contract. Although the gel falls, at the same time it densifies horizontally because bonds relax, not simply due to advection. Collapse is also characterized by a decrease in the surface area of strands to interior strand volume, consistent with ongoing phase separation. Taken together, these changes indicate a re-activated phase separation process. If gel collapse was purely due to gravitational compaction, the network structure would resist collapse. But comparison to a sedimenting suspension of purely repulsive hard spheres revealed that the gel falls more rapidly, because osmotic pressure densifies (collapses) the gel from within by contracting bonds. At long times, the osmotic pressure becomes positive as bonds more fully relax (and some compress), at which point collapse stops. Overall, negative osmotic pressure drives the condensation and once it becomes positive, condensation stops – collapse ends. This prior study provides us with a framework to interrogate the re-activation of phase separation in the context of our view of non-equilibrium phase separation in colloidal gels. We now seek a more general view of osmotic pressure as the driver of non-equilibrium phase separation in gels under shear or startup flow.

4.3 Delayed yield of colloidal gels under fixed stress

Here we turn our attention to reversible-gel yield under a fixed, imposed shear stress, and examine it for hallmarks of re-initiated phase separation. While any gel – including those with very strong interparticle bonds – can fluidize when sheared by a sufficiently strong stress, here we restrict our attention to the behavior gels with of $5kT - 10kT$ bonds, where stresses much weaker than thermal fluctuations trigger yield. The ultimate fate of a reversible colloidal gel subjected to fixed shear stress is determined by the strength of the applied stress; with weak imposed stress, it can remain solid, creeping but never flowing; subjected to strong stress, it can creep, yield, then fluidize; but for intermediate applied stress, the flowing gel can resolidify. In our prior work we placed these regimes on a phase map and demonstrated a precise correspondence to the microscopic evolution: net bond gain to creep, net bond loss to fluidization, and a reversal from loss to gain that signified macroscopic re-solidification. [22] The re-solidification behavior suggested that in fact the mechanical yield, flow, re-solidification may be non-equilibrium phase behavior, given the similarity to the slow compaction regime in gravitational collapse. Further, the reversal to bond gain during re-solidification is characterized by potential energy indicative of free energy minimization via the formation and relaxation of bonds, the key state variable we observe on the march towards phase separation. In the present study of delayed yield, we use simulations to measure the structural evolution and osmotic pressure and the framework we have developed thus far. We then use these findings to determine whether delayed yield is in fact release from kinetic arrest and, if so, if the evolution of osmotic pressure is the underlying driving force.

One hallmark of phase separation found in our prior study [22] emerged from post-yield structural evolution. As the colloidal gel coarsens during flow, the gel becomes strong enough to resist flow and elastic behavior returns. This re-solidification occurs when net bond loss reverses to net bond gain, and gives a connection to phase separation: net formation of bonds is consistent with an increase in the number of deeply buried particles compared to surface particles (an increase in volume to surface-area ratio). This connection is strengthened by examining the evolution of static structure factor, $S(q)$, Figure 5 (c) which exhibits a peak that moves to smaller wavenumbers (indicating a growth in characteristic lengthscale) — and ultimately becomes immeasurably small, indicative of a smoother interface between the dilute and condensed regions. Moreover, the gel occupies a new position in the phase diagram that could not have been reached via the qui-

escent coarsening path. We cannot easily decouple the two con-

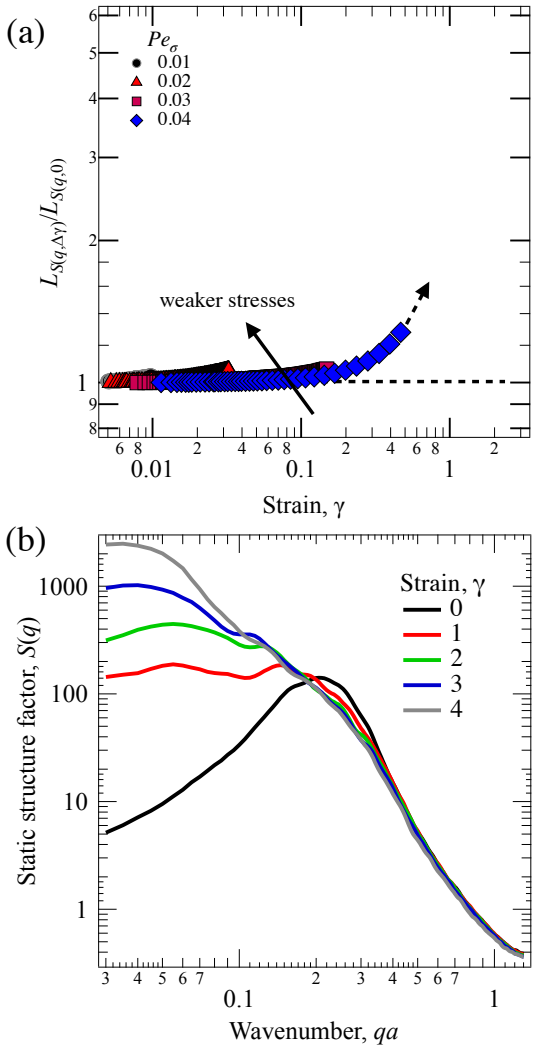

Fig. 5 (a) Normalized dominant length scale as a function of strain for several Pe_σ (from Landrum, Russel & Zia[22], with permission). (b) Static structure factor $S(q)$ plotted as a function of wavenumber q at several strains for $Pe_\sigma = 0.754$. Both plots are shown for a gel with $5kT$ attractions and an age of 40,000 a^2/D prior to the step stress.

tributions to this condensation (as we could in gravitational collapse): that which is driven purely by advection, and that which is driven by osmotic pressure. But we recall that the shear stress is weaker than Brownian motion and much weaker than interparticle attractions. This in itself suggests that the disruption of glassy arrest spurs the already-present negative osmotic pressure to drive deformation, and the shear stress simply gives some weak directionality to the condensation. Here, we examine the osmotic pressure as a possible underlying driving force.

In the present simulations, we examine the osmotic pressure as it evolves concomitantly with the previously reported potential energy and structural evolution, 6. Osmotic pressure is initially negative as described in Section 4.1 as for a quiescently aged gel. As the gel creeps, the osmotic pressure weakens faster compared to quiescent aging. Meanwhile, the potential energy is nearly constant. Close to the yield point, the osmotic pressure begins to weaken more rapidly, consistent with a release from arrest and re-initiated phase separation. During flow, the average osmotic pressure grows less negative, suggesting that osmotic pressure acts to condense the gel by relaxing bonds. It would be easy to naïvely assume that the flow simply pushes bulk strands into contact where new bonds relax and reduce the osmotic pressure. But advection is quite weak relative to Brownian motion, and the bulk deformation of the gel is quite small at yield (Figure 6,inset); in contrast, the osmotic pressure is $O(kT)$. In addition, Brownian motion has been shown to facilitate yield[22]. Together these facts show that the gel condenses due to bond formation and relaxation driven primarily by osmotic pressure, which was liberated as a driving force when the few bonds were lost at yield. This picture is consistent with the idea of re-activated phase separation.

Subsequently, the osmotic pressure abruptly weakens just prior to macroscopic re-solidification, indicating that osmotic pressure drives re-solidification. During re-solidification, the potential energy shows a reversal to increasing bond formation, suggesting that with a weakened negative osmotic pressure, phase separation re-arrests. The applied stress eventually triggers a secondary yield, and the cycle continues.

4.4 Yield of colloidal gels during imposed deformation

Forcing a gel to deform via an imposed strain rate can lead to interesting time-dependent behaviors such as stress overshoots, stress oscillations, and thixotropy.[18,25,39,40] The flow energy accumulates in the gel, resulting in a gradual climb to peak stress. In a previous simulation study we showed that stress builds partly because interparticle bonds stretch and store energy[25], and that when the gel reaches a maximum capacity to store flow energy as stretched bonds, it yields. However, yield need not require network failure but can result when just a few bonds break. As the stress decreases following the yield peak, there is a cascade of bond relaxation with only minor bond loss, and the gel flows. The fact that this can occur due to perturbation much weaker than

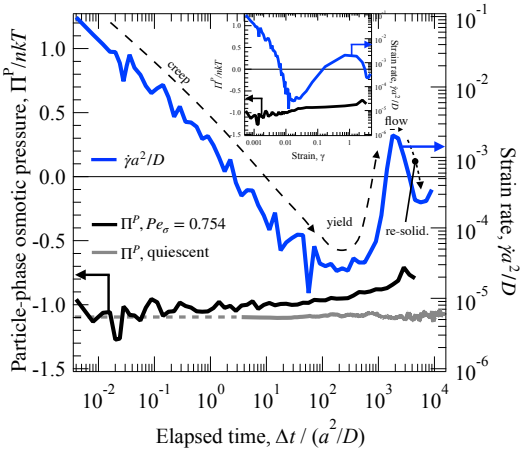

Fig. 6 Particle-phase osmotic pressure and strain rate as a function of time (inset, function of strain) for a gel under step stress of $Pe_\sigma = 0.754$ for a $5kT$ gel with an initial age of 40,000 a^2/D. Grey curve is the osmotic pressure of the quiescent gel with dashed line to guide the eye to its value at times smaller than a time resolution of 4 a^2/D.

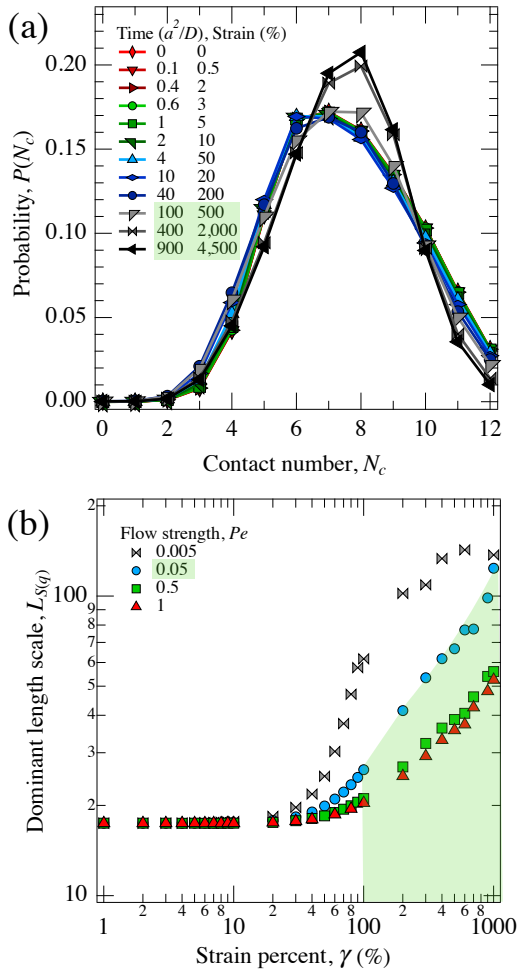

Fig. 7 (a) Contact number distribution at several strains after the application of a strain rate of strength $Pe_{\dot{\gamma}} = 0.05$. (b) Dominant length scale $L_{S(q)}$ as a function of strain percent for several $Pe_{\dot{\gamma}}$. Both plots are shown for gels with $6kT$ attractions aged to $4,000a^2/D$ prior to the application of a step strain rate.

Brownian motion suggests that the external perturbation cannot be solely responsible for yield. Bond loss can later reverses to bond gain as the gel continues to deform. Concomitantly, the post-yield stress decay reverses and increases again. The fact that this occurs under weak flow suggests advection is not the primary driver of the growth in particle rich regions but rather that, as with the gravitational collapse and delayed yield, it liberates negative osmotic pressure that condenses the gel as bonds relax. We test that idea here and its connection to re-initiated phase separation. Figure 9.

One hallmark of phase separation is the minimization of surface area relative to the volume of densely packed colloids. In the present study we monitor the surface area to volume ratio via the contact number distribution and the evolution of the dominant length scale, plotted in Figure 7 (a) and (b). During an imposed shear strain, the contact-number distribution shifts weakly left after the peak stress, consistent with minor bond loss at yield. However, this trend in $P(N_c)$ appears to reverse at the same deformation (∼100-200%) at which the net number of contacts begins to increase: there is a marked increase in the number of deeply buried particles ($N_c \geq 7$), with a concomitant decrease in the number of surface particles ($1 \leq N_c \leq 6$), indicating a decrease in the surface-area to volume ratio, consistent with condensation. Prior to yield, the length scale of the gel is unchanged for all flow strengths but grows after yield (cf Figure 7 (b)). The strain at which the increase commences is well after yield, and corresponds to the increase in shear stress, suggesting condensation. If this condensation is due to advection, then for $Pe_{\dot{\gamma}} = 1$, there should be similar increases in length scale. However, neither of these is the case; in fact, the length scale growth is slower for stronger flow. Together these suggest that another mechanism drives the condensation. Given our findings above that osmotic pressure drives condensation in quiescent coarsening, collapse, and delayed shear yield, we examine osmotic pressure as the potential driving force for this behavior.

We plot the osmotic pressure as it evolves with the shear stress in Figure 8. There seem to be contradictory trends in osmotic pressure and shear stress during the early flow startup. The shear stress suggests accumulated energy stored in stretched bonds. Meanwhile, the osmotic pressure becomes less negative, which indicates average bond relaxation and energy release. To reconcile these two measurements, we recognize that although flow energy was stored in stretched bonds, there is both an extensional axis and a compressional axis in shear flow, leading to a significant number of compressed bonds. Yield takes place when flow energy can no longer compress or stretch bonds. As a result, the osmotic pressure gets a negative contribution from many stretched bonds and a nearly equal but slightly smaller positive contribution from slight bond compression. The osmotic pressure can thus be decomposed into that arising from very compressed bonds interior to the strands and the stretching bonds on the network surface. The interior of the strands is already phase separated; but it is the surface of the gel where phase separation can continue, and there we find a negative osmotic pressure. At the yield point, the osmotic pressure become strongly negative again because the over-compression of the strand interiors relaxes and many bonds are lost. As deformation continues, the osmotic pressure takes over, relaxing many bonds to coarsen the gel. As those bonds relax, the osmotic pressure weakens. The two measurements, osmotic pressure and shear stress, reveal two different driving forces: the $O(kT)$ osmotic pressure, acting to relax bonds (which act normally between particles), and the substantially weaker $<< kT$ imposed flow, acting to separate bonds along the extensional axis. Altogether the evolution of contact number, length scale, potential energy and stress suggest that osmotic pressure acts to condense the gel by relaxing bonds which subsequently allows new bonds to form. Reactivated phase separation and re-solidification can thus be disentangled from the changes in structure or bond distribution imposed by the very weak external flow. That is, the $<< kT$ weak advection acts primarily to trigger a release of glassy frustration imparted by the quiescently aged initial structure and permit a more rapid condensation than possible without disrupting glassy arrest.

Overall we have attributed changes in the osmotic pressure to microstructural evolution and thus reveal the mechanistic role

of osmotic pressure during deepening arrest, release from arrest, and re-activated phase separation which further cements the idea that the osmotic pressure is the intrinsic driving force for gel evolution.

4.5 Osmotic pressure from a microscopic perspective

Here we seek to connect the macroscopic driving force, the osmotic pressure, to the micromechanical mechanism of coarsening, which is the continuous diffusive ratcheting of particles into ever more-bonded, deeper energy states. As the gel quiescently arrests, glassy frustration keeps bonds stretched, unable to relax, locking away the remaining osmotic pressure until external perturbation permits them to relax, liberating the osmotic pressure. To connect this to phase separation, here we focus on how each population of particles — binned by contact number — contribute to the total particle-phase osmotic pressure. Again we emphasize that our results, analysis, and conclusions pertain to moderately-concentrated to dense, hard-sphere colloidal gels formed by short-ranged attractions of $5kT$ to $10kT$. Long-range attractions, or attractions with a very strong primary minimum exhibit distinct phenomenology both during gelation and thereafter.

The bulk osmotic pressure discussed thus far is the volume average of all the individual particle contributions. The number and length of bonds each particle has affects its contribution or partial pressure. Here, we measure the partial pressure of each contact number population as the weighted contribution of each population to the bulk osmotic pressure. As a result, we can identify which contact number populations, and therefore which regions of the colloidal gel are responsible for changes in bulk osmotic pressure.

We plot the partial pressure measured in simulation in the present study as a function of contact number alongside the contact number distribution $P(N_c)$ in Figures 10 (a) and (b). Particles with seven or fewer contacts exhibit negative osmotic pressure over all ages. These populations, $N_c \leq 7$ are the most mobile and carry out the surface diffusion – the coarsening mechanism revealed in our prior work[14] – and this is supported from a driving force perspective in this work. However, the surface populations decrease in size over time. Further, this weakening of osmotic pressure at the strand surfaces signifies smoothing of the energy landscape, i.e., self-limiting coarsening into deeper arrest. The negative osmotic pressure gets transferred to the interior of the gel and the "driving force" gets locked away and cannot be used. Over time, there are many deeply-buried particles in the condensed region, where bonds remain stretched because particles are sterically constrained. Although there is osmotic pressure "present" to condense the gel, it is not "available" until a "kick" releases this arrest. We can examine the evolution in partial pressure under external forcing to see if this microscopic look at the driving force does indeed reveal that a release of the negative osmotic pressure stored from the quiescent aging process is connected to yield and re-invigoration of aging.

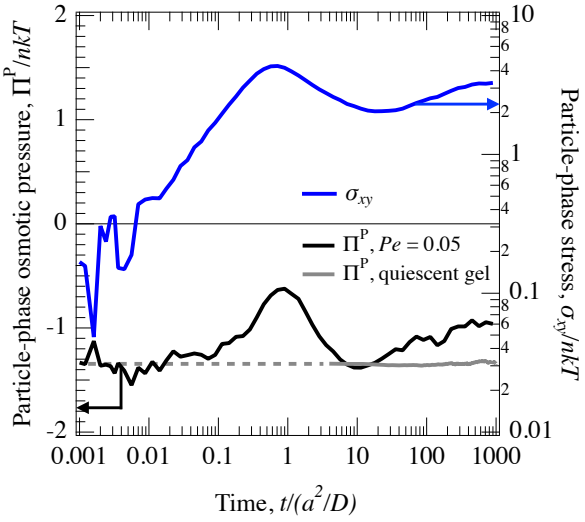

Fig. 8 Particle-phase osmotic pressure and strain rate as a function of time for a gel under step shear strain rate of strength $Pe_{\dot{\gamma}} = 0.05$ for a $6kT$ gel aged to 4,000 a^2/D prior to the application of the strain rate. Grey curve is the osmotic pressure of the quiescent gel with dashed line to guide the eye to its value at times smaller than a time resolution of 4 a^2/D.

We showed in our prior work on gravitational collapse that the gradient of the osmotic pressure across the thickness of the strand weakens as the weak external forcing disrupts the glassy arrest and allows many bonds to relax, Figures 10 (c) and (d).[24] At times prior to and during the rapid collapse, and in the middle layer of the gel, all contact number groups undergo fluctuations in the value of the partial pressure although the sign remain negative for all but the highest contact numbers as the bonds throughout the thickness of the colloidal gel relax and drive densification. Once a substantial jump towards a coarser gel has occurred, collapse slows when this osmotic pressure gradient weakens. We take from this rapid and more global weakening in the osmotic pressure the conclusion that gel collapse harnessed the the osmotic pressure locked in the frustrated/jammed interior particles as well as surface particles to rapidly condense the network from within, resulting in collapse that subsequently slows as the driving force (osmotic pressure) decays. We next examine how the signatures of the partial pressure change when a shear stress is imposed. We present the partial pressure and contact number distribution as the gel evolves under a constant shear stress in Figures 10(e) and (f). At the yield point, the partial pressure and contact number distribution are similar to the initial values prior to applying the shear stress. During flow and leading up to re-solidifcation, some bonds are lost as shown by the shift in contact number to the left. Yet, during flow, the osmotic pressure of the surface and embedded particles weaken in their contributions to osmotic pressure suggesting that many bonds are relaxing that were once held in place by glassy frustration. As the partial pressures weaken, the strain rate slows, suggesting gradients in the osmotic pressure drive flow, and that weakening of these gradients will prompt re-arrest/re-solidification. We next view the re-arrest and resistance to continued deformation from the view of a constant deformation rate where such changes manifest as a shear stress. We find the partial pressure and contact number distribution of a gel subjected to a fixed strain rate exhibit a

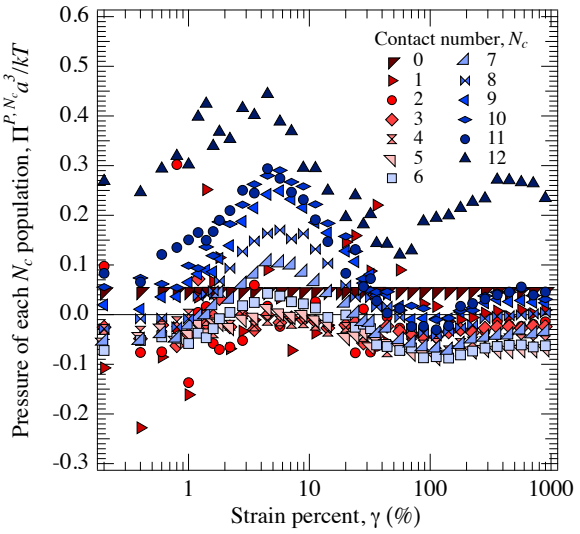

Fig. 9 Osmotic pressure of each contact number population as a function of strain percent for a gel with $6kT$ attractions and an age of 4,000 a^2/D prior to strain rate of $Pe_{\dot{\gamma}} = 1$.

similar trend, Figures 10(g) and (h). Under a steady strain rate, the stress buildup to yield that causes the osmotic pressure to become less negative is again shown to arise from compression in the condensed region (more highly bonded particles) in the gel. The small loss in bonds at yield results in a slight shift left in the contact number distribution. Post-yield, the osmotic pressure contributions from surface particles and moderately bonded particles weakens while deeply buried particles, which initially exhibit positive osmotic pressure, begin to exhibit less positive pressure. Such a change in partial pressure suggests that the relaxation of bonds initiated by the yield point releases deeply buried particles from a frustrated glassy state which had become stuck or frozen-in during quiescent aging. As the strain rate continues to deform the gel at long times, the shear stress increases. Concomitantly, the contact number distribution shifts to the right signaling net bond formation and the partial pressure gradients flatten as seen in the delayed yield case. This suggests a step forward in phase separation has occurred arising from a bulk relaxation of the gel that followed the disruption of glassy frustration that occurred at yield.

Overall, we have presented a framework that casts the structural and rheological evolution of reversibly bonded colloidal gels as a non-equilibrium phase separation during arrest and once released from arrest by external forcing. Osmotic pressure is the driver. Gradients in the partial osmotic pressure in a quiescently aged gel are sharp and reveal that the negative osmotic pressure is locked away progressively with ongoing coarsening. When external forcing can provide just a very weak “kick", bulk relaxation occurs throughout the thickness of gel strands and permit the osmotic pressure to re-activate post yield. Coarsening slows again as the gradients in osmotic pressure weaken and the gel may re-arrest.

5 Conclusions

We have presented a framework to view the evolution of reversibly bonded colloidal gels as ongoing non-equilibrium phase separation. Our results, analysis, and conclusions pertain to moderately-concentrated to dense, hard-sphere colloidal gels formed by short-ranged attractions of $5kT$ to $10kT$, where bond rupture from thermal fluctuation is frequent. In our series of simulation studies, we observe gel evolution under quiescent conditions[14] and in response to weak fields, forces, or flow.[22,24,25] We focus on two macroscopic hallmarks of phase separation: increases in surface-area to volume ratio that accompanies condensation, and minimization of free energy, and we form connections to mechanical stress and bond dynamics. Here, we measured the osmotic pressure and its partial pressure binned by contact number to identify it as a driver for phase separation.

Our prior study of age coarsening showed that gels formed by arrested phase separation may not actually be arrested, because they age under quiescent conditions – that is, they may still be undergoing some non-equilibrium phase separation process. Aging was previously demonstrated by a growth in the characteristic network length scale and the formation and growth of dense, glassy strands accompanied by a decrease in the ratio of the surface area of the strands to volume of strand interiors.[14] Here, we find that the minimization of the free energy, inferred from the potential energy evolution, and a negative bulk osmotic pressure are consistent with ongoing phase separation. We show that the driving force toward phase separation, osmotic pressure, weakens over time: it is self-limiting. Further, the partial pressure contributions to the osmotic pressure show that the march towards lower-energy states may be hindered as the negative osmotic pressure gets locked away inside the strands where the dynamics are arrested.

The picture of gravitational collapse developed in our prior work[24] elucidated the interplay between external forcing and the negative osmotic pressure stored in the gel from quiescent aging. From this basis, we built a framework for re-invigoration and re-arrest of non-equilibrium phase separation as the colloidal gel collapsed from the inside, which comprised surface area minimization, free energy minimization, and a jump forward in coarseness of the gel. First, more negative osmotic pressure was found be associated with the induction of collapse and rapid collapse, revealing negative osmotic pressure as a driving force. Second, the weakening of bulk osmotic pressure, and a weakening in the gradient of osmotic pressure throughout the strand thickness, is associated with the slowing of the sedimentation rate, which can be inferred to drive the re-arrest of phase separation. In this study, we revisited this framework with a view toward establishing yield more generally as release from kinetic arrest and osmotic pressure as the driver of the subsequent non-equilibrium phase separation.

We first looked at delayed yield under a fixed shear stress. New in this study, we measured the osmotic pressure during delayed yield and found that, similar to gravitational collapse, negative osmotic pressure drives phase separation that manifests rheologically as creep, yield, flow and re-solidifcation. In our prior work,[22] we showed that the yield event under step shear stress

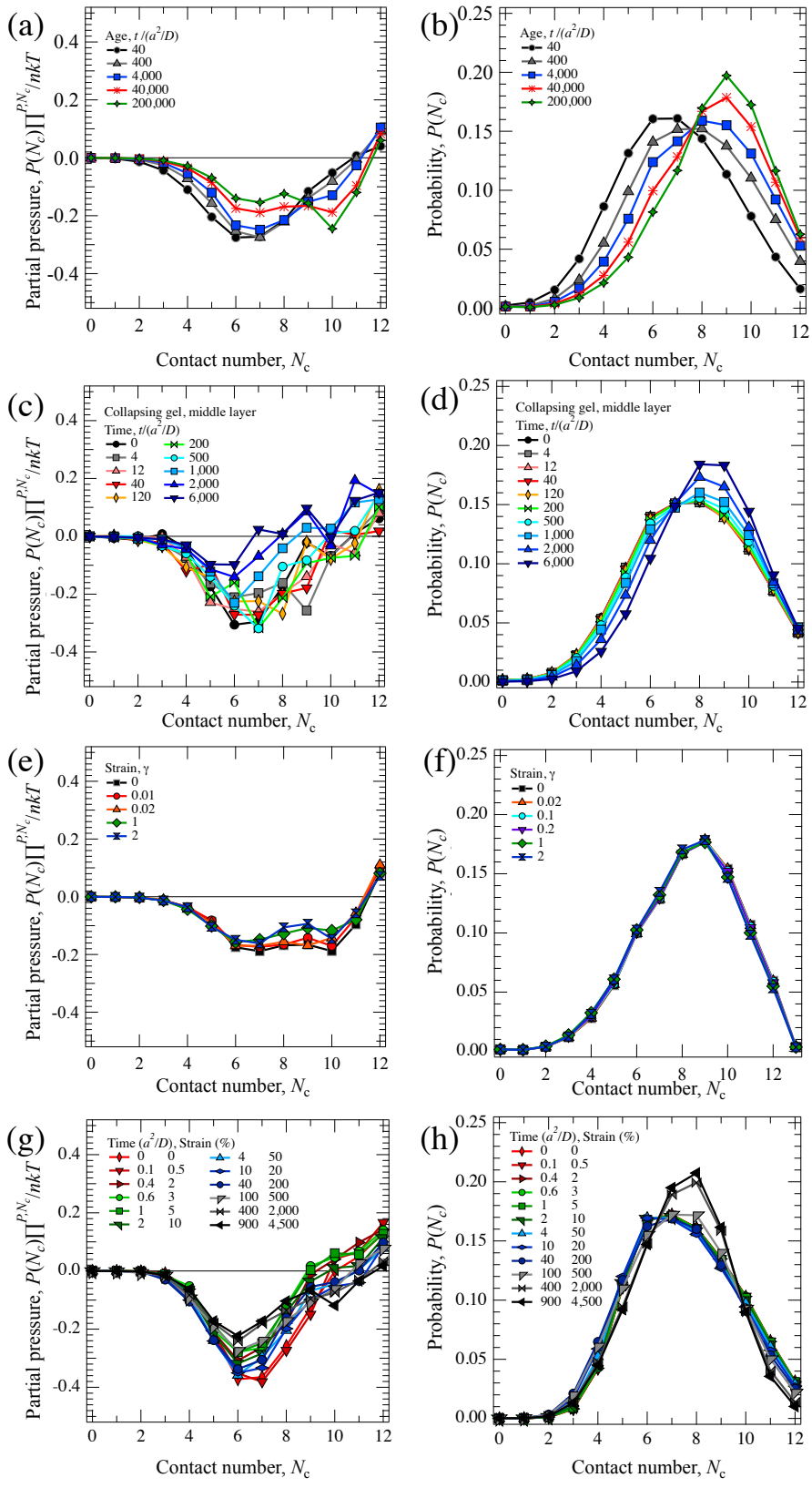

Fig. 10 Partial pressure of each contact number population and contact number distribution for colloidal gels during (a), (b) quiescent aging ($5kT$ attractions at several ages), (c), (d) gravitational collapse ($5kT$ attractions and $Pe_g = 0.05$), (e), (f) delayed yield ($5kT$ attractions, 40,000 a^2/D prior to stress, $Pe_\sigma = 0.754$), and (g),(h) yield under a startup strain rate ($6kT$ attractions, 4,000 a^2/D prior to stress, $Pe_{\dot{\gamma}} = 0.05$). The binned osmotic pressure is weighted by the prevalence of particle type noted in the contact number distribution to compute the partial pressure. Data for (b) reproduced from Zia et al.[14]. Data for (c) and (d) reproduced from Padmanabhan and Zia.[24] Plot (h) is the same as Figure 7(a) and shown here again for clarity.

was characterized by a small loss in bonds that permitted many more to relax, which resulted in macroscopic flow. Concomitant with flow, the gel network coarsens. Such a growth in the network coarseness resists ongoing deformation and eventually the flow ceases as a stronger network emerges and the gel regains elasticity. In the present study, we measured osmotic pressure during delayed shear yield and showed that yield reinvigorates or liberates osmotic pressure, which then drives the enhanced coarsening seen during flow. During flow, the gradients in the osmotic pressure weaken and the gel begins to resolidify, revealing osmotic pressure gradients to be the driving force for these macroscopic condensation behaviors. Combined, these behaviors identify the osmotic pressure as the driver of the delayed yield behavior of colloidal gels.

Next, by imposing a fixed strain rate, we can also recast the findings in our study of startup flow[25] as non-equilibrium phase separation with distinct re-invigoration then re-arresting of rapid phase separation. The cascade of bond relaxation after yield gives a change in potential energy consistent with phase separation.

In the present study, we find that the gel condenses as it deforms: the surface area to volume ratio decreases substantially, another hallmark of phase separation. Upon startup, the bulk shear stress takes builds to a yield peak, at which point a few bonds break and allow many more to relax. An ongoing cascade of bond relaxation lets the gel flow with only minor bond loss. The subsequent growth in gel strength is analogous to resolidification in delayed yield. Our measurements of shear stress, osmotic pressure, and bond dynamics reveal two different driving forces: the $O(kT)$ osmotic pressure, acting to relax bonds (which act normally between particles), and the substantially weaker $\ll kT$ imposed flow, acting to separate bonds along the extensional axis, overall confirming that osmotic pressure rather than advection drives condensation.

The phenomenon we describe here pertains to reversibly bonded gels. For very strongly bonded fractal gels, gel compaction can arise from syneresis, typically described as resulting in expulsion of the suspending fluid, a macroscopic process of a fully-formed gel resulting from a microscopic sintering process where particles get close enough to overcome a soft repulsion and enter into a primary van der Waals minimum and become permanently bonded. Observations of local densification in dilute, fractal gels with bonds $V \gg kT$ have been attributed to a tendency of a system to undergo syneresis that cannot fully take place owing to wall attachment. However, syneresis is not described as occurring alongside or following a phase-separation process, or its arrest, but rather involves the 'curing' of interparticle bonds in a fractal network that does not cause restructuring or coarsening. The role played by wall attachment is to restrict solvent expulsion to localized areas of the gel, resulting in a more fractal network that occupies less volume but remains fractal.[41]. Other explanations of syneresis have sometimes described syneresis as resulting from internal stresses within the gel generated during gelation, but the microscopic origin of these stresses and the reason for their relaxation, are typically not described, leaving open the mechanistic explanation for the phenomenon of syneresis[42]. To our knowledge, such models have focused on low-coordination number gels where single strands stretch and bend; while food-based gels have been the primary focus of gel syneresis, we are not aware of studies of model-system studies of dense, highly-bonded or reversibly-bonded model gels. Syneresis has some parallels to the present work, but here condensation of a reversibly bonded dense gel is shown to emerge from relaxation of bonds and where we provide a microscopic mechanistic explanation: negative osmotic pressure acts to reduce the free energy, advancing phase separation.

In this work, we also developed a micromechanical picture of the partial osmotic pressure by monitoring the pressure contributions from the distinct particle populations on the surface of the gel and embedded within glassy strand interiors. Under quiescent conditions, we find that the surface and moderately bonded particles — which carry out coarsening — contribute to the negative osmotic pressure, but these populations decrease as coarsening progresses. Surface particles become buried in the strands, often with stretched bonds, leaving behind a surface of relaxed bonds. Together the "available" negative osmotic pressure at the surface weakens and much of the driving force of stretched bonds resides in the buried, dynamically slow populations. Experimental measurement of osmotic pressure in a colloidal gel to test these ideas awaits future work. One could imagine placing the gel into another liquid, separated from it by a permeable membrane, or by seeding the gel with bubbles that would compress or expand with changes in osmotic pressure, for example.

We can now view the ongoing aging and flow instabilities of colloidal gels formed by arrested phase separation as being driven by the negative osmotic pressure initially acting to carry out phase separation. The same attractive forces that promote phase separation prevent attainment of an equilibrium arrangement of relaxed bonds as the gel condenses. As a result, negative osmotic pressure accumulates in the gel, locked into the strand interiors in a frozen-in imbalance of attractive and repulsive forces. The interplay between external forcing and Brownian motion induces a yield event that disrupts this glassy frustration, allowing the gel to coarsen rapidly and jump forward in phase separation. We identify this new paradigm for gel aging, yield, and non-equilibrium phase separation as "Phase Mechanics".

Conflicts of interest

There are no conflicts to declare.

Acknowledgements

The authors thank Benjamin Landrum and Poornima Padmanabhan for many insightful conversations, as well as access to data from previous studies. This work was supported by the National Science Foundation Extreme Science and Engineering Discovery Environment (XSEDE) Research Award (No. OCI-1053575) to utilize high-performance computational resources at the Texas Advanced Computing Center (TACC) at the University of Texas at Austin, and by the Office of Naval Research Director of Research Early Career Award, Grant No. N00014-18-1-2105.

Notes and references

1 E. Zaccarelli, *J. Phys.: Condens. Matter*, 2007, **19**, 323101 (1–50).

2 D. A. Weitz and M. Oliveria, *Phys. Rev. Lett.*, 1984, **52**, 1433–1436.

3 W. H. Shih, W. Y. Shih, S.-I. Kim, J. Liu and I. A. Aksay, *Phys. Rev. A*, 1990, **42**, 4772–4779.

4 C. J. Rueb and C. F. Zukoski, *J. Rheol.*, 1997, **41**, 197–218.

5 A. H. Krall and D. A. Weitz, *Phys. Rev. Lett.*, 1998, **80**, 778–781.

6 R. Buscall and L. R. White, *J. Chem. Soc., Faraday Trans. 1*, 1987, **83**, 873–891.

7 C. Kim, Y. Liu, A. Kühnle, S. Hess, S. Viereck, T. Danner, L. Mahadevan and D. A. Weitz, *Phys. Rev. Lett.*, 2007, **99**, 028303.

8 J. J. Liétor-Santos, C. Kim, P. J. Lu, A. Fernández-Nieves and D. A. Weitz, *Eur. Phys. J. E*, 2009, **28**, 159–64.

9 J. Bergenholtz, W. C. K. Poon and M. Fuchs, *Langmuir*, 2003, **19**, 4493–4503.

10 E. Zaccarelli, P. J. Lu, F. Ciulla, D. A. Weitz and F. Sciortino, *J. Phys.: Condens. Matter*, 2008, **20**, 494242(8).

11 M. E. Helgeson, Y. Gao, S. E. Moran, J. Lee, M. Godfrin, A. Tripathi, A. Bose and P. S. Doyle, *Soft Matter*, 2014, **10**, 3122–3133.

12 Y. Gao, J. Kim and M. Helgeson, *Soft Matter*, 2015, **11**, 6360–6370.

13 J. Lu, P, E. Zaccarelli, F. Ciulla, A. B. Schofield, F. Sciortino and D. A. Weitz, *Nature*, 2008, **453**, 499–504.

14 R. N. Zia, B. J. Landrum and W. B. Russel, *J. Rheol.*, 2014, **58**, 1121–1157.

15 W. C. K. Poon, L. Starrs, S. P. Meeker, A. Moussaïd, R. M. L. Evans, P. N. Pusey and M. M. Robins, *Faraday Discuss.*, 1999, **112**, 143–154.

16 R. Buscall, T. H. Choudhury, M. A. Faers, J. W. Goodwin, P. A. Luckham and S. J. Partridge, *Soft Matter*, 2009, **5**, 1345–1349.

17 L. J. Teece, M. Faers and P. Bartlett, *Soft Matter*, 2011, **7**, 1341–1351.

18 N. Koumakis and G. Petekidis, *Soft Matter*, 2011, **7**, 2456–2470.

19 V. Gopalakrishnan and C. F. Zukoski, *J. Rheol.*, 2007, **51**, 623–644.

20 J. Sprakel, S. B. Lindström, T. E. Kodger and D. A. Weitz, *Phys. Rev. Lett.*, 2011, **106**, 248303(4).

21 S. Lindström, T. Kodger, J. Sprakel and D. Weitz, *Soft Matter*, 2012, **8**, 3657–3664.

22 B. J. Landrum, W. B. Russel and R. N. Zia, *J. Rheol.*, 2016, **60**, 783–807.

23 L. Starrs, W. C. K. Poon, D. J. Hibberd and M. M. Robins, *J. Phys.: Condens. Matter*, 2002, 2485–2505.

24 P. Padmanabhan and R. N. Zia, *Soft Matter*, 2018, **14**, 3265–3287.

25 L. C. Johnson, B. J. Landrum and R. N. Zia, *Soft Matter*, 2018, **14**, 5048–5068.

26 D. A. Huse, *Phys. Rev. B*, 1986, **34**, 7845–7850.

27 J. D. Shore, M. Holzer and J. P. Sethna, *Phys. Rev. B*, 1992, **46**, 11376–11404.

28 L. C. Johnson, R. N. Zia, E. Moghimi and G. Petekidis, *Journal of Rheology*, 2019, **63**, 583–608.

29 W. C. K. Poon, A. D. Pirie and P. N. Pusey, *Faraday Discuss.*, 1995, **101**, 65–76.

30 S. Asakura and F. Oosawa, *J. Chem. Phys.*, 1954, **22**, 1255–1256.

31 M. T. Elsesser and A. D. Hollingsworth, *Langmuir*, 2010, **26**, 17989–17996.

32 S. Plimpton, *J Comp Phys*, 1995, **117**, 1 – 19.

33 M. P. Allen and D. J. Tildesley, *Computer simulation of liquids*, Clarendon Press, Gloucestershire", 1987.

34 A. Brünger, C. L. Brooks III and M. Karplus, *Chem. Phys. Lett.*, 1984, **105**, 495–500.

35 D. R. Foss and J. F. Brady, *J. Rheol.*, 2000, **44**, 629–651.

36 W. B. Russel, D. A. Saville and W. R. Schowalter, *Colloidal Dispersions*, Cambridge University Press, 1989.

37 D. J. Evans and G. Morriss, *Statistical Mechanics of Nonequilibrium Liquids*, Cambridge University Press, 2008.

38 N. A. M. Verhaegh, D. Asnaghi, H. N. W. Lekkerkerker, M. Giglio and L. Cipelletti, *Physica A*, 1997, **242**, 104–118.

39 M. Laurati, S. U. Egelhaaf and G. Petekidis, *J. Rheol.*, 2011, **55**, 673–706.

40 J. Colombo and E. Del Gado, *J. Rheol.*, 2014, **58**, 1089–1116.

41 L. Cipelletti, S. Manley, R. C. Ball and D. A. Weitz, *Phys. Rev. Lett.*, 2000, **84**, 2275–2278.

42 Q. Wu, J. van der Gucht and T. E. Kodger, *Phys. Rev. Lett.*, 2020, **125**, 208004.